

Manuscript Number: MARSYS-D-15-00254R3

Title: Effects of physical constraints on the lability of POM during summer in the Ross Sea

Article Type: SI: Ross Sea

Keywords: Particulate organic matter; biochemical composition; phytoplankton biomass; physical structure; Ross Sea; Antarctica

Corresponding Author: Dr. Cristina Misic,

Corresponding Author's Institution: University of Genova

First Author: Cristina Misic

Order of Authors: Cristina Misic; Anabella Covazzi Harriague; Olga Mangoni; Yuri Cotroneo; Giuseppe Aulicino; Pasquale Castagno

Manuscript Region of Origin: ANTARCTICA

Abstract: The 0-200 m surface layer of the Ross Sea was studied during summer 2014 to investigate the lability of the particulate organic matter (POM) in response to physical parameters. With the use of satellite information, we selected three zones, characterised by different physical setting: a northern offshore area, crossing the summer-polynya area of the Ross Sea (hereafter called ROME 1), a more coastal area next to the Terra Nova Bay polynya (ROME 2); a southern offshore area, towards the Ross Ice Shelf (ROME 3). Ice-maps showed that the seasonal ice retreat had already occurred in early December for most of the stations. Statistical analysis of the quantitative and qualitative characteristics of the POM pointed to significant differences between the stations, especially in the upper mixed layer (UML). A comparison with previous studies, showed that the localised pulses of POM accumulation in the UML were similar to those recorded at the highly productive marginal ice zones, providing notable trophic support to the ecosystem. The UML, although rather thin and easily subjected to alterations, confirmed its pivotal role in the ecosystem dynamics. A POM quality favourable to consumers was highlighted at several stations in ROME 1 and ROME 3. Reduced trophic support was, instead, found in ROME 2. A limited POM consumption where deep-water formation takes place, would increase the POM role in the transfer of C to the depths.

Response to Reviewers

Reviewer #2:

All the suggested corrections have been made, we thank Reviewer 2 for the help at improving the text also for language.

Line 50: yes, this was what we meant.

Line 86: the third aim was shortened, avoiding the part that was too much general.

Line 301: a reference has been added.

Line 668: we referred to Table2, that contains all the references to the papers we used for comparison.

Highlights

Highlights of the manuscript “Effects of physical constraints on the lability of POM during summer in the Ross Sea ” by Misic et al.

- 1 The Ross Sea surface layer (0-200 m) was studied during summer 2014
- 2 Particulate organic matter (POM) largely accumulated in the upper mixed layer (UML)
- 3 Mesoscale hydrodynamic features influenced the POM concentrations and lability
- 4 Summer POM lability was favourable to consumers at several offshore stations
- 5 Reduced lability was found coastward, potentially increasing the input of C in the deep-water

1 **Effects of physical constraints on the lability of POM during summer in the Ross Sea**

2

3 Cristina Mistic¹, Anabella Covazzi Harriague¹, Olga Mangoni²,

4 Yuri Cotroneo³, Giuseppe Aulicino³, Pasquale Castagno³

5

6 ¹ Dipartimento di Scienze della Terra, dell’Ambiente e della Vita – University of Genova, C.so Europa 26, 16132 Genova, Italy

7 ² Dipartimento di Biologia, University of Napoli Federico II, Via Mezzocannone, 8, 80134 Napoli, Italy.

8 ³ Dipartimento di Scienze e Tecnologie, University of Napoli Parthenope, Centro Direzionale di Napoli IS. C4, 80143 Napoli, Italy

9

10

11

12

13 Corresponding author:

14 Cristina Mistic,

15 Dipartimento di Scienze della Terra, dell’Ambiente e della Vita - University of Genova

16 C.so Europa 26, 16132 Genova, Italy.

17 Phone: +3901035338224, e-mail: mistic@dipteris.unige.it

18

19 **Abstract**

20 The 0-200 m surface layer of the Ross Sea was studied during summer 2014 to investigate the lability of the
21 particulate organic matter (POM) in response to physical parameters. With the use of satellite information,
22 we selected three zones, characterised by different physical setting: a northern offshore area, crossing the
23 summer-polynya area of the Ross Sea (hereafter called ROME 1), a more coastal area next to the Terra
24 Nova Bay polynya (ROME 2); a southern offshore area, towards the Ross Ice Shelf (ROME 3). Ice-maps
25 showed that the seasonal ice retreat had already occurred in early December for most of the stations.
26 Statistical analysis of the quantitative and qualitative characteristics of the POM pointed to significant
27 differences between the stations, especially in the upper mixed layer (UML). A comparison with previous
28 studies, showed that the localised pulses of POM accumulation in the UML were similar to those recorded
29 at the highly productive marginal ice zones, providing notable trophic support to the ecosystem. The UML,
30 although rather thin and easily subjected to alterations, confirmed its pivotal role in the ecosystem
31 dynamics. A POM quality favourable to consumers was highlighted at several stations in ROME 1 and ROME
32 3. Reduced trophic support was, instead, found in ROME 2. A limited POM consumption where deep-water
33 formation takes place, would increase the POM role in the transfer of C to the depths.

34

35 **Key Words**

36 Particulate organic matter, biochemical composition, phytoplankton biomass, physical structure, Ross Sea,
37 Antarctica

38

39 **1. Introduction**

40 Particulate organic matter (POM) is operationally defined as any material that does not pass through a
41 given filter, usually 0.45-1 μm (Volkman and Tanoue, 2002; Verdugo et al., 2004). POM includes detrital
42 matter as well as living organisms. Ice-algae, phytoplankton, nano- and microzooplankton, and
43 mesozooplankton-derived particles are included in POM, as well as bacteria adhering on particles.

44 In the Antarctic Ocean, the quantitative features of the POM have been extensively studied using *in-situ*
45 bottle and pump sampling and remote-sensing techniques (especially chlorophyll-a and particulate organic
46 carbon - POC) (e. g. Smith et al., 2000; Smith and Asper, 2001; Lee et al., 2012; Arrigo et al., 2012; Schine et
47 al., 2016), while detailed information on its biochemical composition and nutritional value for consumers is
48 less abundant (e. g. Rossi et al., 2013; Soares et al., 2015; Kim et al., 2016).

49 In addition to the ratios that are commonly used to infer the value of POM as a trophic resource (for
50 instance the POC/PON ratio and the POC/chlorophyll-a ratio), other analyses focusing on the caloric
51 content and hydrolysable fractions of the POM can be useful (Fabiano et al. 1993; Fabiano and Pusceddu,
52 1998; Misic and Covazzi Harriague, 2008; Kim et al., 2014). Caloric content expresses the general value of
53 POM in energy terms. Different biochemical compositions result in quantitatively different energy values
54 for POM. For the hydrolysable fraction, potential biomimetic assays have been developed to evaluate the
55 fraction that may be rapidly hydrolysed by enzymes commonly found in the environment; these assays
56 estimate the actual fraction of POM that is bioavailable to consumers. This approach, although testing only
57 a few of the enzymes actually active in the environment, by-passes the uncertainty of bulk-related analyses
58 (such as POC). The biomimetic assay allows for the possibility that some compounds may be biochemically
59 refractory to consumption, or physically enclosed in low-lability materials that isolate them from
60 consumers.

61 The Antarctic Ocean and the Ross Sea are characterised by interannual, seasonal and spatial variability of
62 biological features (Smith et al., 1996; Arrigo et al., 1998; Dunbar et al., 1998; Gardner et al., 2000;
63 Saggiomo et al., 2002; Smith et al., 2010; Fragoso and Smith, 2012), whose forcing mechanisms are still
64 largely unclear. Among others, the ice presence regulates the onset of primary production, POM

65 accumulation and distribution in the water column (Garrity et al., 2005). The ice presence or absence
66 influence the water column properties, determining the depth of the upper mixed layer (UML) that is often
67 considered to be a major factor in controlling POM production and distribution (Mangoni et al., 2004;
68 Frago and Smith, 2012). Therefore, based on the degree of maturity of the selected ice-system, a typical
69 evolution scheme may be defined (Fabiano et al., 2000): closed pack conditions, followed by the Marginal
70 Ice Zone (MIZ) spring conditions, and then by open waters in late spring and summer. This occurs, generally
71 in the offshore area by late December and in the entire continental shelf region by late January (Comiso et
72 al., 1993, Smith and Asper, 2001). Once the ice is melted in summer, other forces can influence the
73 planktonic patterns. Although ice may last longer at some sites in the Ross Sea, depending on global climate
74 anomalies as well as local events (Arrigo and van Dijken, 2004), the summer features of the Ross Sea should
75 show less variability than the spring ones. The stratification generated by ice melting should be relaxed due
76 to wind and waves on the open waters, a feature that would allow increased vertical water mixing and a
77 more homogeneous vertical distribution of the POM (Gardner et al., 2000).

78 This study is based on the results of the ROME (Ross Sea Mesoscale Experiment) cruise, carried out during
79 the Antarctic summer of 2014. Sampling focused on the 0-200 m surface layer of three locations in the Ross
80 Sea, characterised by different distances from the coast and different mesoscale hydrodynamic structures.

81 We aimed to: i) highlight whether the quantitative and qualitative features of the POM were homogeneous
82 and the potential effects of physical constraints in the sampled areas, ii) test whether our summer POM
83 features resembled those of previous research performed in the Ross Sea, iii) underline the potential role
84 of the POM as trophic resource.

85

86 **2. Material and methods**

87 *2.1 Station sites and sampling*

88 *The in situ* ROME data were collected by the R/V *Italica* in the framework of the Italian National Program for
89 Antarctic Research (PNRA). Sampling was performed in three different areas of the Ross Sea: ROME 1 was
90 sited at approximately 170°E and 75°S; ROME 2 occupied a more coastward area, next to the Terra Nova

91 Bay (TNB) polynya; ROME 3 was placed in the southern Ross Sea, towards the Ross Ice Shelf, at ca. 168°E
92 (Fig. 1A).

93 The sampling strategy was defined using the sea surface temperature and surface chlorophyll-a
94 concentration maps from MODIS (Moderate Resolution Imaging Spectroradiometer) Aqua and Terra
95 satellite level-2 products for the previous 12/24 hours. The goal was to carry out bottle casts where both
96 high and low chlorophyll occurred. Additionally, satellite AMSR2 sea ice concentration maps, provided by
97 the University of Bremen, using the ASI sea ice concentration algorithm (Spreen et al., 2008), were
98 considered. Daily maps of the Ross Sea region from early December 2013 to late February 2014 (available
99 at <http://www.iup.uni-bremen.de:8084/amsr2>) were analyzed to monitor the evolution of the sea ice cover
100 before and during the experiment.

101 A total of 46 casts were conducted. Hydrological profiles were acquired by means of a SBE 9/11 Plus CTD,
102 with double temperature and conductivity sensors. For each station the upper mixed layer (UML) depth
103 was determined as the depth at which *in situ* density (σ_t) changed by 0.05 kg/m³ over a 5 m depth interval.
104 Current speed and direction were recorded using a Lowered Acoustic Doppler Current Profiler (LADCP)
105 system. Two LADCP were deployed with the CTD, in order to obtain a unique current measurement every
106 10 m from the surface to the maximum depth reached. The effect of tides on the current dataset was
107 removed following the procedure proposed by Erofeeva et al. (2005).

108 Water samples for phytoplankton biomass and POM analysis were collected at 21 stations (Table 1, black
109 circled stations in Fig. 1A) using a Carousel sampler equipped with 24 Niskin bottles (12 L).

110 For the POM analysis, water samples were collected at 4 fixed depths (surface, 50, 100 and 200 m) and 1
111 variable depth depending on the maximum of the signal for fluorescence. From 0.5 to 1 L of sampled
112 seawater was filtered through Whatman GFF filters (25 mm, nominal pore diameter 0.7 μ m) and
113 immediately frozen until analysis in the laboratory. For the total phytoplankton biomass analysis, the
114 samples were filtered and quickly stored at -80 °C until analysis.

115

116 *2.2 Analytical procedures*

117 The amount of phytoplankton biomass was estimated from spectrofluorometric analysis on acetone-
118 extracted chlorophyll-a, following Holm Hansen et al. (1965). The extract was read using a Varian Eclipse
119 spectrofluorometer, which was checked daily with a chlorophyll-a standard solution (from *Anacystis*
120 *nidulans* by Sigma). The specific standard deviation of the replicates was based on an average of 4%.

121 Particulate organic carbon (POC) and particulate organic nitrogen (PON) were analyzed following Hedges
122 and Stern (1984), after acidification with HCl fumes, in order to remove inorganic carbon. Cyclohexanone 2-
123 4-dinitrophenyl hydrazone was used to calibrate a Carlo Erba Mod. 1110 CHN Elemental Analyser. The
124 specific standard deviations due to the analytical procedures and sample handling were 7.4% and 7.8% for
125 POC and PON, respectively.

126 Particulate protein, carbohydrate and lipid concentrations were analyzed following Hartree (1972), Dubois
127 et al. (1956), Bligh and Dyer (1959) and Marsh and Weinstein (1966). Albumin, glucose and tripalmitine
128 solutions were used to calibrate a Jasco V530 spectrophotometer. The specific standard deviations were
129 8.3%, 15.5% and 21.6% for the proteins, carbohydrates and lipids, respectively.

130 The concentrations of proteins, carbohydrates and lipids were used to estimate the caloric value of the
131 POM (Kcal g POM⁻¹) following the Winberg (1971) equation (Kcal g POM⁻¹ = 0.055 protein% +0.041
132 carbohydrate% + 0.095 lipid%).

133 The enzyme-hydrolysable fractions of particulate proteins and carbohydrates were determined following
134 the protocols of Gordon (1970), Mayer et al. (1995) and Dell'Anno et al. (2000). The sample filters and filter
135 blanks (Whatman GFF filters not used for filtration) were placed in plastic containers with solutions (100 mg
136 l⁻¹ in 0.1 M Na-phosphate buffer) of two selected enzymes purchased from Sigma–Aldrich. Proteinase K was
137 chosen for the hydrolysis of the proteins, β-glucosidase for that of the carbohydrates (Mayer et al., 1995,
138 Dell'Anno et al., 2000). These enzymes are extracted from plants and fungi, but have hydrolytic activities
139 quite similar to natural marine organisms and are widespread among autotrophs and heterotrophs (Dall
140 and Moriarty, 1983). The filters were left in the enzyme solutions for 2 hours, at the optimal temperatures
141 and pH for each enzyme, in order to enhance digestion (Dell'Anno et al., 2000). After hydrolysis, each filter
142 was carefully removed from its container, placed in a filter-holder and rinsed with the solution remaining in

143 the dish and 5ml of deionised water, to return any particles that may have floated off the filter (Gordon et
144 al., 1970). After that, the filters were processed for the determinations of protein and carbohydrate
145 concentrations as above. The possibility that the flushing of the buffer could have mechanically removed
146 part of the particulate fraction was avoided by incubating and processing replicates of the samples with
147 only the buffer solution. In addition, an underestimate of the labile proteins and carbohydrates was
148 possible due to the sorption to minerals or POM (and therefore to their return to the particulate fraction)
149 of the hydrolysed materials. The concentrations detected after hydrolysis, corrected for the eventual error
150 just mentioned (never higher than 20% of the total protein and carbohydrate concentrations), were
151 subtracted from the total concentrations in order to obtain the hydrolysable, or labile, POM. The specific
152 standard deviations were 11.2% and 21.5% for hydrolysable particulate proteins and carbohydrates,
153 respectively.

154

155 *2.3 Data treatment and statistical analysis*

156 The POM data were divided into a surface layer, defined by the UML depth (Table 1), and a deeper layer,
157 ranging from the UML depth down to 200 m.

158 Published data related to previous researches carried out in the Ross Sea and TNB were used for
159 comparison. In particular, POC, protein and carbohydrate spring concentrations for the Ross Sea were
160 provided by Fabiano et al. (2000), while early summer data were found in Fabiano et al. (1993) and
161 Catalano et al. (1997). Summer data for the TNB area have been published by Fabiano et al. (1995 and
162 1997) and Povero et al. (2001) (Table 2).

163 We tested the significance of differences in each variable between different samplings with the one-way
164 ANOVA test followed by the Newman-Keuls *post-hoc* test (ANOVA-NK test) (Statistica software). To test the
165 relationships between the various parameters, a Spearman-rank correlation analysis was performed.

166 Principal Component Analysis (PCA) was applied to the normalised POC, protein and carbohydrate
167 concentrations and the protein/carbohydrate ratio (PRIMER software). The data were divided into the UML
168 and the deeper layer, as previously described. The ROME data were treated together with the other

169 literature data previously cited (Table 2) to highlight similarities between them. Cluster analysis was
170 performed on the normalised data set (resemblance measure: Euclidean distances, cluster mode: group
171 average), to visually highlight the station grouping. The analysis of similarities (ANOSIM) was applied to
172 highlight significant differences between the groups, while the similarity percentage analysis (SIMPER) was
173 utilised to highlight the parameters responsible for such differences.

174

175 **3. Results**

176 *3.1 Physical properties and sea-ice conditions*

177 The Θ/S diagram obtained from all the sampled stations (Fig. 1B) indicated the presence of several typical
178 Ross Sea shelf water masses. In all the studied areas the surface layer was occupied by Antarctic Surface
179 Water (AASW), a relatively light surface water characterized by potential temperatures ranging between -
180 1.8°C and $+1^{\circ}\text{C}$ and by salinity values lower than 34.50 (Orsi and Wiederwohl, 2009). In ROME 2 (blue circles
181 in Fig. 1B), the AASW core was slightly saltier and denser than expected, with salinity close to 34.60. These
182 values were similar to the Modified Circumpolar Deep Water (MCDW) features, but the high oxygen
183 concentration values (Rivaro et al., 2015) confirmed that we were in the presence of a local AASW.

184 The intermediate and deep layers (from 150 to 1000 m) were occupied by High Salinity Shelf Water (HSSW),
185 and by Terra Nova Bay Ice Shelf Water (TISW), the latter identified only in ROME 2 (Fig. 1B). HSSW is
186 characterized by salinity greater than 34.70, potential temperature near the freezing point and potential
187 density greater than 27.9 kg/m^3 (Budillon et al., 2003; Rivaro et al., 2014). TISW (from 150 to 350 m) is
188 characterized by potential temperatures below freezing point and salinity values of about 34.70 (Budillon
189 and Spezie, 2000).

190 The physical properties of the upper layer may also be linked to sea ice evolution in the study area. The
191 melting ice in the Ross Sea gradually generates large ice-free areas during summer. Some ROME 1 and
192 ROME 3 stations and all the ROME 2 stations experienced ice-free conditions starting from early December
193 (Figs. 2A and 2B). On the other hand, some stations experienced a longer ice presence (Figs. 2C and 2D).
194 Even in the same sampling area, differences in ice cover can be significant and have an impact on the

195 observed temperature and salinity values. For instance, the northernmost station of ROME 1 (station 20)
196 was covered by ice until 14 January, just 3 days before the sampling. Stations 16 and 18 started to become
197 ice-free from the beginning of January (Fig. 2C). The ROME 3 stations were partially covered by ice just until
198 the end of December (Fig. 2B).

199 The vertical structure of the water column of ROME 1 showed deeper UMLs for the stations that
200 experienced longer ice-free conditions (9, 11 and 13, Table 1). In the western stations of ROME 1 the lower
201 depth of the mixed layer depended on the presence of low-salinity surface water, related to the influence
202 of the ice (Fig. 3A). Intensity and direction of the currents along the entire water column (mean UML
203 shown in Fig. 3C) showed the presence of a northward current along the eastern and western boundary of
204 the leg, while more intense southward velocities were registered in the central part of the leg (stations 13
205 and 14).

206 The ROME 2 water column was characterized by a UML depth limited to the first 10-15 m (Table 1) due to
207 the presence of a salinity and temperature gradient between the fresher and colder coastal stations and
208 the easternmost, saltier and warmer stations (Figs. 3D and 3E). A frontal structure was visible in the area
209 between stations 45 and 34, where the convergence of the two water masses led to a deepening of the
210 thermocline down to 100 m (Rivaro et al., 2015) and to an abrupt change in the current pattern (Fig. 3F).

211 The strongest current intensities ($p < 0.05$) were observed in ROME 3, with values up to 24 cm sec^{-1} for the
212 zonal (u) and meridional (v) components. The current pattern at all depths showed the presence of a
213 cyclonic circulation centred at about $168.5^\circ\text{E } 76.45^\circ\text{S}$ (Fig. 3I). This circulation could have increased the UML
214 water mixing, leading to salinity values of 34.23-34.43 and mean temperature values lower than 0.5°C (Figs.
215 3G and 3H). In fact, the western and central stations (48, 50, 55, 67 and 75) had a more homogeneous
216 water structure for the upper 30-50 m, while stations, placed outside the eddy showed higher surface
217 salinity values and the deepest UML (more than 70 m).

218

219 *3.2 Particulate organic matter*

220 The concentration and distribution of chlorophyll-a in the three areas (see Table in appendix) varied with
221 the physical setting. In ROME 1 the stations characterised by early ice melting showed rather homogeneous
222 chlorophyll-a concentrations in the UML, ranging from 1 to 2 $\mu\text{g l}^{-1}$. Instead, where the halocline was
223 shallower and the stratification stronger (i.e. station 16), a subsurface increase in concentration up to 3 μg
224 l^{-1} was observed, leading to higher average values. The chlorophyll-a distribution in ROME 2 was influenced
225 by the previously described hydrological front (Figs. 3D and 3E), associated with the deepening of the
226 thermocline at stations 34 and 45. The frontal structure and the current convergence allowed high
227 chlorophyll-a concentrations at higher depths (values up to 3 $\mu\text{g l}^{-1}$ at 100 m, data not shown). In ROME 3
228 the stations directly influenced by the cyclonic eddy (55, 67 and 75) showed the highest mean chlorophyll-a
229 concentrations, with maximum values higher than 4 $\mu\text{g l}^{-1}$.

230 POC values correlated significantly with chlorophyll-a concentrations in ROME 1 and ROME 3 (Table 3).
231 ROME 2, instead, showed no significant correlation, although at 50 and 100 m depths significantly higher
232 POC concentrations ($p < 0.05$) than the other two areas were found (Fig 4A).

233 The POC/chlorophyll-a ratio is an indication of the primary biomass contribution to the total POM. The
234 ratios (see Table in appendix) highlighted a generally lower contribution of the photoautotrophic
235 component at the UMLs of ROME 1 and 2, with ratio higher than 150, especially in the stations
236 experiencing longer ice-free conditions (stations 9 and 11 of ROME 1, for instance). In ROME 3 the lowest
237 ratio was, instead, found for the stations lying to the west of the frontal zone.

238 PON and POC concentrations were strongly correlated (Table 3), indicating similar distributions (Figs. 4A
239 and 4B) and likely origins. POC/PON ratios showed variations with depth (Fig 4C); this ratio gives an
240 estimate of the N contribution to the bulk POM, an indication of lability given that N-containing molecules
241 are considered attractive to consumers (Huston and Deming, 2002). The highest POC/PON ratios (above 8)
242 were found in the deeper water layers, especially at stations 9 and 11 in ROME 1 and 50, 52, 56, 69 and 75
243 in ROME 3. The lowest values, below 6, were, instead, found in the UML, especially in ROME 3, where the
244 highest chlorophyll-a values were found. However, significant chlorophyll-a and POC/PON ratio correlations

245 were only found in ROME 2, although this relationship ($r= 0.48$, $n=19$, $p<0.05$) highlighted that an increase
246 of autotrophic biomass led to a lowering of the trophic value of the POM.

247 On average, the protein and carbohydrate concentrations showed vertical trends very similar to those of
248 POC (Figs. 4D and 4G), and significant correlations were found between these variables for the three areas
249 (Table 3). Proteins and carbohydrates also correlated with chlorophyll-a in ROME 1 and 3, while no
250 significant correlation was found in ROME 2. Furthermore, the hydrolysable fraction of the carbohydrates
251 and lipids was not coupled with the other variables in ROME 2. A reduction of the hydrolysable
252 carbohydrates was, in fact, observed starting from 100 m (Fig. 4H). In this area the lipid concentrations (Fig.
253 4I) did not show significant decreases with depth (UML vs. deeper layer, $p>0.05$) but rather similar values,
254 significantly lower than in the other areas ($p<0.001$). The contribution of the three POM fractions to POC
255 was reported in Fig. 5A for the UML and the deeper layer. Generally, higher concentrations of residual POC
256 (here called "other POC") were found at the UML, except for stations 34 and 45, that showed a high
257 residual POC fraction also in the deeper layer.

258 On average, the hydrolysable proteins were $35.4\pm 11.7\%$ of the total proteins (ranging from 6.8 to 75.6%),
259 the hydrolysable carbohydrates $13.1\pm 10.8\%$ of the total carbohydrates (ranging from 0.1 to 44.9%).
260 Generally, the deeper layer contribution of the hydrolysable proteins to POC was higher than the UML one,
261 except for the front-related stations in ROME 2 and station 20 in ROME 1 (Fig 5A). The hydrolysable
262 carbohydrate contribution to POC (Fig.5B) was lower and showed a higher variability in the three areas. In
263 ROME 1, for instance, the contribution showed an inverse trend with chlorophyll-a. The 200-m-deep
264 contributions were higher at the stations not covered by ice from a longer time, than at the stations more
265 recently influenced by ice. ROME 3, however, showed a rather good relationship between the hydrolysable
266 carbohydrate and the phytoplanktonic biomass. The large variability of the hydrolysable carbohydrate
267 contribution to the POC concentration, often visible in Fig. 5B as high standard deviation, implied also
268 strong variations within the UML and the deeper layer that were not found for the hydrolysable proteins.

269

270 *3.3 Multivariate statistical analysis*

271 PCA results are shown in Fig. 6, where the cluster analysis is shown as ellipses defined by Euclidean
272 distances. The PC1 axis explained 71% of the variation, while the PC2 explained a further 24%. Two
273 significantly different main groups (ANOSIM analysis, Table 4) were observed: the main part of the UML
274 observations belonged to the richer group A, while the deeper layer observations were clustered in group
275 B. Proteins and carbohydrates explained the major part of this difference (SIMPER analysis, Table 4). The
276 group B stations showed POC concentrations 3.4-fold lower than the observations of group A, 4.8 for
277 proteins and 2.8 for carbohydrates.

278 In group A the samples were organised into two main sub-groups: a1 and a2. The multivariate analyses
279 highlighted significant differences between them (ANOSIM analysis, Table 4), mainly due to the different
280 ratios between proteins and carbohydrates (explaining 41% of the difference, SIMPER analysis, Table 4). In
281 group B two more sub-groups were recorded, differing significantly (ANOSIM analysis, Table 4) due to the
282 carbohydrate concentrations (explaining 47% of the difference, SIMPER analysis, Table 4).

283 Each sub-group had a particular signature, defined by the previous studies carried out in the area (Table 2):
284 sub-group a1 clustered the MIZ stations (8, 10, 28, 30) and the spring polynya station MP, sub-group a2 the
285 coastal TNB stations. The surface observations characterised by a closed-pack coverage (27 and 29)
286 belonged to sub-group b1, together with the main part of the deeper layer observations; sub-group b2
287 collected those of the early summer polynya stations (15, 17, 19, 21) and the deeper coastal layer
288 observations (TNB).

289

290 *3.4 Caloric value analysis*

291 The caloric value of the POM in the two water layers was only calculated for stations where the lipid
292 analysis was carried out, namely 9, 13, 16 and 20 of ROME 1, 34, 39 and 45 of ROME 2 and 50, 55 and 67 of
293 ROME 3. The plot of these results, with the previous research carried out in the Ross Sea and at the coastal
294 TNB (Table 2) is presented in Fig. 7. In this figure we have merged the bulk quantitative (POC) and
295 qualitative (caloric value) information on the POM.

296 During previous research (Fabiano et al., 2000), a rising trend was noticed for POM concentrations in the
297 UML from the poorer pack-ice zones to the polynya and then to the MIZ, ending with the richer coastal
298 sites, although the MIZ could also show high concentrations of POM of moderate caloric values. The
299 previous pack-ice observations (Fabiano et al., 1993) showed that low concentrations were associated with
300 an average caloric value, while the qualitative value of the other stations was higher (MIZ and coastal) or
301 lower (polynya).

302 The stations in ROME 2 matched the quantitative and qualitative features of the polynya in the entire water
303 column. The surface observations of the other areas were grouped with the MIZ and previous coastal
304 observations for the UML. The deeper layer observations in the ROME 1 and ROME 3 areas resembled
305 those of the MIZ, spring polynya and deeper pack-layer, although their caloric value was higher.

306

307 **4. Discussion**

308 *4.1 Quantitative and qualitative features of the summer POM and a comparison with previous studies in the* 309 *Ross Sea*

310 Focusing on the quantitative characteristics of POM at different stations (PCA -multivariate analysis, Fig. 6),
311 we observed significant quantitative differences between the two water layers (Table 4), with a sharp
312 reduction in POM in the deeper layer, as already established by the observations by Nelson et al. (1996),
313 Fabiano et al. (2000) and Gardner et al. (2000) for the Ross Sea. They stated that the primary production is
314 recycled in the photic layer, following the concept of a “retentive system”. The grouping of the
315 observations of the two layers, as revealed by multivariate analysis, indicated a strong and significant
316 variability in the UML, while the deeper layer was more homogeneous in the ROME study area, also when
317 compared to observations from other years and seasons, except for the ROME 2 stations influenced by the
318 frontal area.

319 Ice-free water conditions were established in the whole ROME sampling area from the beginning of January
320 (with the exception of the northern station of ROME 1), at least two weeks before the sampling. Therefore,
321 open water conditions, resembling those of the previous spring-summer polynya/open water observations,

322 were common in the entire area. Actually, the multivariate analysis performed on the UML POM indicated
323 a higher similarity to the spring MIZ zones studied in the previous published researches than to the summer
324 polynya ones. Several processes, due to the peculiar physical features as well as biological, may be
325 responsible of such similarity, irrespective of the ice dynamics.

326 In our study, an example of the strict relationship between physical forcing, phytoplankton biomass and
327 POM accumulation was provided by ROME 3, where a clear cyclonic circulation was observed. In this case,
328 the UML depth (generally deeper than 30 m in our study) exerted a lower influence on the POM production
329 and accumulation than that observed by Fragoso and Smith (2012), who noted that the shallower mixed
330 layer depths (<20 m) in late spring and early summer appeared to promote diatom growth. In our study,
331 the water mixing of the UML, due to the more intense hydrodynamic forcing, fertilised the surface layer,
332 probably stripped of nutrients by earlier spring blooms. In addition, a higher instability in the water column,
333 that is known to influence phytoplankton development, could have favoured some species that, before,
334 were limited by competition (Fonda Umani et al., 2002).

335 The phytoplankton biomass was pivotal for the POM composition. In fact, it regulated the POM
336 quantitative features, as revealed by the highly significant correlations between the chlorophyll-a and the
337 quantitative variables of the POM (Table 3) (Davis and Benner, 2005) and by the POC/chlorophyll-a ratio
338 values for the stations on the western side of the area (eddy-influenced zone), that were significantly lower
339 ($p < 0.05$) than the other ROME areas. Young et al. (2015) found that Antarctic diatoms take up to 50% of
340 biomass to protein, explaining the very high significance of the correlation. Arrigo and van Dijken (2004)
341 described the area of ROME 3 as a boundary between spring and summer blooms, a kind of frontal area
342 that may show an unusually high chlorophyll-a accumulation at the surface, depending on general
343 atmospheric conditions over the entire Ross Sea.

344 Our observations point to the pivotal role of the summer autotrophic processes, providing a large
345 accumulation of biomass and strongly sustaining the ecosystem. This feature was unclear in the multi-year
346 comparison by Arrigo and van Dijken (2004) and in the studies by Smith and Asper (2001) and Rigual-
347 Hernandez et al. (2015), who observed a general decrease in chlorophyll-a concentrations from spring to

348 summer in normal years. In addition, the POC/chlorophyll-a ratios of our study were significantly lower
349 ($p < 0.05$) than those reported by Smith et al. (2000) for the Ross Sea in summer, while they were similar to
350 the values the same authors reported for spring. This confirmed the pivotal role of the living phytoplankton
351 fraction during summer in the UML of the Ross Sea, where mesoscale hydrological structures occur.

352 The sub-group a1 of the PCA linked some stations of the ROME cruise and the previously studied spring
353 polynya station MP and spring MIZ ones. The MIZ stations are generally characterised by high POM
354 productivity (Saggiomo et al., 1998; Fitch and Moore, 2007), being the priming for further planktonic
355 development. The multivariate statistical analysis confirmed that these stations had rather high POM
356 concentrations and, in particular, they showed the highest prevalence of proteins over carbohydrates, a
357 signal of recent production (Pusceddu et al., 2000). It is well known that N-rich proteins cover multiple roles
358 (energetic, functional, structural) and thus a high protein concentration indicates a good food supply for
359 consumers (Etcheber et al., 1999), especially in the upper water column. Particulate carbohydrates,
360 instead, generally have a lower lability, because they also encompass complex structural polysaccharides
361 whose digestion is energy-expensive, slowing their consumption rates (Pusceddu et al., 2000). One of the
362 main processes that enrich the POM of proteins is microbial activity. Microbial heterotrophic reworking of
363 autotrophic and detrital POM, generally performed by bacteria, increases the N content of the detritus
364 (Povero et al., 2003) and of the autotrophic colonies (Carlson et al., 1998) especially during summer. A
365 general and marked dominance of proteolysis over other classes of hydrolytic enzymes has been previously
366 reported (Misic et al., 2002; Celussi et al., 2009), indicating an efficient N-recycling by unicellular
367 heterotrophs. The conversion of detrital-N into high trophic value biomass is completed by an efficient
368 microbial-loop, recovering a large part of the DOM released during phytoplanktonic blooming (Kirchman et
369 al., 2001). In addition, Sala et al. (2005) found that bacteria might utilise other DOM sources (in particular
370 dissolved carbohydrates), thus increasing their efficiency in biomass accumulation. The rather low
371 POC/PON ratio values we found compared, for instance, to Smith et al. (2000) (on average for the upper
372 100 m layer they found summer values of 6.9 ± 0.5 vs. our 5.8 ± 0.3 and 6.4 ± 0.9 calculated for the UML and 0-
373 200 m layer, respectively), are consistent with micro-heterotrophic presence, as bacterial standing stock

374 can be considered as the amount of particulate organic matter possessing high nutritional quality
375 (Monticelli et al., 2003).

376

377 *4.2 Caloric value of summer POM*

378 The plotting of the POC with the POM caloric value (Fig. 7) provides information on the energy potentially
379 available for the heterotrophic consumers by the POM. The ROME stations that resemble the spring and
380 early-summer features of the polynya were those of ROME 2. Actually, these stations experienced real
381 polynya environmental conditions, being next to the TNB polynya.

382 The ROME 2 stations had low caloric values in the entire water column, although, from a quantitative point
383 of view, some of them in the UML had similar features to the richer coastal areas (sub-group a2 of Fig 6). In
384 the entire water column, POM maintained the same caloric content of the mixed layer, as previously found
385 for the coastal TNB (Fabiano et al., 1996), when the caloric value was on average 5.33 Kcal/g. This is not
386 really very high, due to the high contribution of carbohydrates that have the lowest caloric value among the
387 three biochemical components. We observed that in ROME 2 the chlorophyll-a was associated with
388 carbonaceous POM (it correlated positively to the POC/PON ratio), therefore in this area the freshly-
389 produced summer POM had different features, namely a lower trophic value, than the offshore area.

390

391 *4.3 Hydrolysable proteins and carbohydrates of summer POM*

392 Generally, the hydrolysable protein contribution was on average 35% of the total proteins during the ROME
393 cruise. This was clearly lower than the contribution (higher than 90%) observed at coastal stations in the
394 NW Mediterranean (Misic and Covazzi Harriague, 2008), and by Fabiano and Pusceddu (1998), who
395 observed that 50% of the total proteins in TNB were hydrolysable. Besides the possibility that actual
396 variations in time and space may occur, these differences may be due to the fact that the cited authors
397 used trypsin to hydrolyse proteins, while in the present study, we used proteinase K. The hydrolysable
398 carbohydrate contribution to total carbohydrates, instead, showed average values similar to those
399 recorded in the previously cited NW Mediterranean (from 5 to 30%), but notably lower than the 80% found

400 in TNB using the same method and hydrolytic enzyme. This pointed to sharp spatial variations of the
401 hydrolysable fraction of POM from the actual coastal area (Fabiano and Pusceddu, 1998) to the offshore
402 area next to the polynya of TNB (this study). The vertical trends of the hydrolysable carbohydrates in the
403 three ROME areas were different, reflecting a general influence by the environmental features on the
404 distribution of the hydrolysable carbohydrate, but the relatively small size of our data set prevented deeper
405 analysis of this item.

406 The main contribution to POC was given by the hydrolysable proteins, that showed slight, but interesting
407 differences between the ROME areas and in the same area, following the mesoscale physical features.

408 Assuming that the POM production in the Ross Sea has a main phytoplankton signature (Fragoso and Smith,
409 2012), the fresh (generally more labile) POM should be found at the surface at the beginning of the
410 productive season (spring), but the water vertical mixing of summer and the proliferation of the bacterial
411 biomass would increase the quantity of labile heterotrophic materials such as proteins in the depth.

412 At the ROME sites the contribution of the labile proteinaceous C to the POC was, generally, higher in the
413 deeper layer than in the mixed layer (Fig. 5A). In ROME 1 this proved true for the stations that had
414 experienced longer ice-free conditions. Generally, in such areas, the relaxing of the stratification due to
415 wind and waves allows a more homogeneous vertical distribution of POM by water-mass physical mixing.
416 The lower maturity of station 20 (namely a higher ice-influence as revealed by salinity), instead, led to
417 conditions more similar to spring, with a higher labile contribution at the surface.

418 ROME 2, instead, showed peculiar features. Despite being ice-free for the longest time and lying next to the
419 winter polynya of TNB, its stations displayed a lower labile contribution in the deeper layer than in the
420 UML. Station 39 was an exception, lying to the east of the hydrological front and being influenced by an
421 offshore current coming from the ROME 1 area. The other stations were separated from the actual offshore
422 area by the front found at stations 34 and 45.

423 The vertical transport of the POM by vertical water mixing has a double relevance: it is essential for the
424 foraging of bottom and mesopelagic communities, and it may contribute to the CO₂ biological pump. The
425 occurrence of vertical transport, as shown by the ROME 2 and coastal observations in terms of bulk POM,

426 may improve deep-sea nutrition, but also push C into the deep current system via the bottom-water. The
427 vertical distribution of POM at the ROME 2 stations pointed to an efficient biological pump, because the
428 POM accumulation was observed down to 200 m. The TNB area is characterised by the formation of dense
429 water masses due to brine release during sea-ice production (HSSW) and by the freshening and cooling of
430 the HSSW due to contact with the ice shelf (TISW). HSSW fills-up the deeper layer of the Drygalsky Basin
431 and flows northwards until it reaches the shelf-break, which overflows down the continental slope,
432 ventilating to the abyssal depths near Cape Adare (Jacobs et al., 1970; Withworth and Orsi, 2006; Budillon
433 et al., 2011). The deep layer POM of ROME 2 was more refractory, showing proportionally lower
434 hydrolysable proteins and carbohydrates, higher POC/PON ratio, lower protein/carbohydrate ratio and a
435 lower caloric content than the mixed layer. If refractivity is a limiting factor for the biological respiration of
436 POM, it allows a more efficient burial of not respired C to the depth, indicating TNB as a sink for C in
437 summer (Fonda Umani et al., 2002).

438

439 **5. Conclusions**

440 In this study, we firstly aimed at determining whether the POM was uniformly distributed in the Ross Sea
441 area during a particular season (summer), when one of the main constraints regulating POM production
442 and consumption (namely the ice cover) was generally lacking. We found that heterogeneity was still a
443 dominant feature of the Ross Sea, due to the mesoscale characteristics of each area. The presence of fronts
444 and eddies, with high current intensities, mixed the UML, stimulating phytoplankton production and POM
445 accumulation. Nevertheless, the vertical and horizontal extent of this fertilisation was not continuous. The
446 offshore ROME 1 and 3 areas differed from the ROME 2 area, especially with regards to the qualitative
447 features of the POM. The deeper-layer POM was found to have higher lability in ROME 1 and 3, while the
448 more coastal ROME 2 had inverse features. This may be relevant, because the POM of the deeper water,
449 which would likely join the dense-water journey to the abyssal depths of the oceans, has a potentially lower
450 trophic value and could be respired to a lesser extent, contributing to C storage in the bottom. On the other
451 hand, enrichment of the deeper POM of the other areas via bacterial growth and high protein-containing

452 phytoplankton would increase its trophic value, providing a valuable source of materials and energy for
453 those consumers that also maintain a certain metabolic activity during winter.

454 This study also highlighted that the heterogeneity of the offshore areas was principally a matter of the
455 UML. This is a critical point, because the surface layer is the first to be influenced by climatic changes. Small
456 atmospheric changes could lead to increased ecological changes, altering the fragile balance of the
457 Southern Ocean.

458

459 **Acknowledgements**

460 We would like to thank the captain and crew of the R/V *Italica* for their unstinting assistance during the
461 cruise. We are grateful to Paolo Povero and Enrico Olivari for their logistical support and for the hard
462 sampling work, to Paola Rivaro, who provided the UML depths, and to Giorgio Budillon for the constructive
463 discussion on the physical data. This study was conducted in the framework of the project “Ross Sea
464 Mesoscale Experiment (ROME)” funded by the Italian National Program for Antarctic Research (PNRA,
465 2013/AN2.04).

466

467 **References**

- 468 Arrigo, K.R., Worthen, D., Schnell, A., Lizotte, M.P., 1998. Primary production in Southern Ocean Waters. *J.*
469 *Geophys. Res.* 103, 15587–15600.
- 470 Arrigo, K.R., Lowry, K.E., vanDijken, G.L., 2012. Annual changes in sea ice and phytoplankton in polynyas of
471 the Amundsen Sea, Antarctica. *Deep-Sea Res. II* 5, 71–76.
- 472 Arrigo, K.R., van Dijken, G.L., 2004. Annual changes in sea-ice, chlorophyll a, and primary production in the
473 Ross Sea, Antarctica. *Deep-Sea Res. I* 51, 117–138.
- 474 Bligh, E.G., Dyer, W.J., 1959. A rapid method of total lipid extraction and purification. *Can. J. Biochem.*
475 *Physiol.* 37, 911–917.
- 476 Budillon, G., Spezie, G., 2000. Thermohaline structure and variability in the Terra Nova Bay polynya, Ross
477 Sea. *Antarct. Sci.* 12, 493–508.

478 Budillon, G., Castagno, P., Aliani, S., Spezie, G., Padman, L., 2011. Thermohaline variability and Antarctic
479 bottom water formation at the Ross Sea shelf break. *Deep-Sea Res. Part I*, 1002–1018.

480 Budillon, G., Pacciaroni, M., Cozzi, S., Rivaro, P., Catalano, G., Ianni, C., Cantoni, C., 2003. An optimum
481 multiparameter mixing analysis of the shelf waters in the Ross Sea. *Antarct. Sci.* 15,105-118.

482 Carlson, C.A., Ducklow, H.W., Hansell, D.A., Smith, W.O., 1998. Organic carbon partitioning during spring
483 phytoplankton blooms in the Ross Sea polynya and the Sargasso Sea. *Limnol Oceanogr.* 43 (3), 275-
484 386.

485 Catalano, G., Povero, P., Fabiano, M., Benedetti, F., Goffart, A., 1997. Nutrient utilisation and particulate
486 organic matter changes during summer in the upper mixed layer (Ross Sea, Antarctica). *Deep-Sea*
487 *Res. I* 44, 97–112

488 Celussi, M., Cataletto, B., Fonda Umani, S., Del Negro, P., 2009. Depth profiles of bacterioplankton
489 assemblages and their activities in the Ross Sea. *Deep-Sea Res. I* 56, 2193–2205.

490 Comiso, J.C., McClain, C.R., Sullivan, C.W., Ryan, J.P., Leonard, C.L., 1993. Coastal Zone Color Scanner
491 pigment concentrations in the Southern Ocean and relationships to geophysical surface features. *J.*
492 *Geophys. Res.* 98, 2419-2451.

493 Dall, W., Moriarty, D.J.W., 1983. Functional aspects of nutrition and digestion. In: Mantel, L.H. (Ed.), *The*
494 *Biology of Crustacea*, vol. 5. Academic Press, New York, pp. 215–261.

495 Davis, J., Benner, R., 2005. Seasonal trends in the abundance, composition and bioavailability of particulate
496 and dissolved organic matter in the Chukchi/Beaufort Seas and western Canada Basin. *Deep-Sea Res.*
497 *II* 52, 3396–3410.

498 Dell’Anno, A., Fabiano, M., Mei, M.L., Danovaro, R., 2000. Enzymatically hydrolysed protein and
499 carbohydrate pools in deep-sea sediments: estimates of the potentially bioavailable fraction and
500 methodological considerations. *Mar. Ecol. Progr. Ser.* 196, 15–23.

501 Dubois, M., Gilles, K.A., Hamilton, J.K., Rebers, P.A., Smith, F., 1956. Colorimetric method for determination
502 of sugars and related substances. *Anal. Chem.* 39, 350-356.

503 Dunbar, R.B., Leventer, A.R., Mucciarone, D.A., 1998. Water column sediment fluxes in the Ross Sea,
504 Antarctica: atmospheric and sea ice forcing. *J. Geophys. Res.* 103 (30), 741-759.

505 Erofeeva, S.Y., Egbert, G.D., Padman, L., 2005: Assimilation of ship-mounted ADCP data for barotropic tides:
506 Application to the Ross Sea, *J. Atmos. Oceanic Technol.*, 22: 721-734.

507 Etcheber, H., Relexans, J.-C., Beliard, M., Weber, O., Buscail, R., Heussner, S., 1999. Distribution and quality
508 of sedimentary organic matter on the Aquitanian margin (Bay of Biscay). *Deep-Sea Res.* 46, 2249-
509 2288.

510 Fabiano, M., Pusceddu A., 1998. Total and hydrolyzable particulate organic matter (carbohydrates, proteins
511 and lipids) at a coastal station in Terra Nova Bay (Ross Sea, Antarctica). *Polar Biol.* 19,125-132.

512 Fabiano, M., Povero, P., Danovaro, R., 1993. Distribution and composition of particulate organic matter in
513 the Ross Sea (Antarctica). *Polar Biol.*13, 525–533.

514 Fabiano, M., Danovaro, R., Crisafi, E., La Ferla, R., Povero, P., Acosta-Pomar, L., 1995. Particulate matter
515 composition and bacterial distribution in Terra Nova Bay (Antarctica) during summer 1989-1990.
516 *Polar Biol.* 15, 393-400.

517 Fabiano, M., Povero, P., Danovaro, R., 1996. Particulate organic matter composition in Terra Nova Bay (Ross
518 Sea, Antarctica) during summer 1990. *Antarct. Sci.* 8, 7–13.

519 Fabiano, M., Chiantore, M., Povero, P., Cattaneo-Vietti, R., Pusceddu, A., Misic, C., Albertelli, G., 1997.
520 Short-term variation in particulate matter flux in Terra Nova Bay, Ross Sea. *Antarct. Sci.* 9, 143-149.

521 Fabiano, M., Povero, P., Misic, C. 2000. Spatial and temporal distribution of particulate organic matter in
522 the Ross Sea. In Faranda, F.M., Guglielmo, L., Ianora, A. (Eds.) *Ross Sea ecology*. Berlin: Springer, pp.
523 135–150.

524 Fitch, D. T., Moore, J. K., 2007. Wind speed influence on phytoplankton bloom dynamics in the Southern
525 Ocean Marginal Ice Zone, *J. Geophys. Res.* 112, C08006, doi:10.1029/2006JC004061.

526 Fonda Umani, S., Accornero, A., Budillon, G., Capello, M., Tucci, S., Cabrini, M., Del Negro, P., Monti, M., De
527 Vittor, C., 2002. Particulate matter and plankton dynamics in the Ross Sea Polynya of Terra Nova Bay
528 during the austral summer 1997/1998. *J. Mar. Syst.* 36, 29–49.

529 Fragoso, G.M., Smith Jr., W.O., 2012. Influence of hydrography on phytoplankton distribution in the
530 Amundsen and Ross Seas, Antarctica. *J. Mar. Syst.* 89, 19–29.

531 Gardner, W.D., Richardson, M.J., Smith Jr., W.O., 2000. Seasonal patterns of water column particulate
532 organic carbon and fluxes in the Ross Sea, Antarctica. *Deep-Sea Res.* 47, 3423-3449.

533 Garrity, C., Ramseier, R.O., Peinert, R., Kern, S., Fischer, G., 2005. Water column particulate organic carbon
534 modeled fluxes in the ice-frequented Southern Ocean. *J. Mar. Syst.* 56, 133– 149.

535 Gordon Jr., D.C., 1970. Some studies on the distribution and composition of particulate organic carbon in
536 the North Atlantic Ocean. *Deep-Sea Res.* 17, 233–243.

537 Hartree, E.F., 1972. Determination of proteins: a modification of the Lowry method that gives a linear
538 photometric response. *Anal. Biochem.* 48, 422–427.

539 Hedges, J.I., Stern, J.H., 1984. Carbon and nitrogen determination of carbonate-containing solids. *Limnol.*
540 *Oceanogr.* 29, 657–663.

541 Holm-Hansen, O., Lorenzen, C.J., Holmes, R.W., Strickland, J.D.H., 1965. Fluorometric determination of
542 chlorophyll. *J. Cons. Perm. Int. Explor. Mer.* 30, 3-15.

543 Jacobs, S.S., Amos, A.F., Bruchhausen, P.M., 1970. Ross Sea oceanography and Antarctic Bottom Water
544 formation. *Deep-Sea Res.* 17, 935–962.

545 Kim, B.K., Lee, J.H., Yun, M.S., Joo, H.T., Song, H.J., Yang, E.J., Chung, K.H., Kang, S.-H., Lee, S.H., 2014. High
546 lipid composition of particulate organic matter in the northern Chukchi Sea, 2011. *Deep- Sea Res. II*,
547 120, 72-81. DOI: 10.1016/j.dsr2.2014.03.022i

548 Kim, B.K., Lee, J.H., Joo, H.T., Song, H.J., Yang, E.J., Lee, S.H., Lee, S.H., 2016. Macromolecular compositions
549 of phytoplankton in the Amundsen Sea, Antarctica. *Deep-Sea Res. II* 123, 42-49.

550 Kirchman, D.L., Meon, B., Ducklow, H.W., Carlson, C.A., Hansell, D.A., Steward, G.F., 2001. Glucose fluxes
551 and concentrations of dissolved combined neutral sugars (polysaccharides) in the Ross Sea and Polar
552 Front Zone, Antarctica. *Deep-Sea Res. II* 48, 4179–4197.

553 Lee, S.H., Kim, B.K., Yun, M.S., Joo, H., Yang, E.J., Kim, Y.N., Shin, H.C., Lee, S., 2012. Spatial distribution of
554 phytoplankton productivity in the Amundsen Sea, Antarctica. *Polar Biol.* 35,1721–1733.

555 Mangoni, O., Modigh, M., Conversano, F., Carrada, G.C., Saggiomo, V. 2004. Effects of summer ice coverage
556 on phytoplankton assemblages in the Ross Sea, Antarctica. *Deep-Sea Res. I* 51 (11): 1601-1617.

557 Marsh, J.B., Weinstein, D.B., 1966. A simple charring method for determination of lipids. *J. Lipid Res.* 7, 574-
558 576.

559 Mayer, L.M., Schick, L.L., Sawyer, T., Plante, C.J., Jumars, P.A., Self, R.L., 1995. Bioavailable amino acids in
560 sediments: a biomimetic, kinetics, based approach. *Limnol. Oceanogr.* 40, 511–520.

561 Mistic, C., Covazzi Harriague, A., 2008. Organic matter recycling in a shallow coastal zone (NW
562 Mediterranean): the influence of local and global climatic forcing and organic matter lability on
563 hydrolytic enzyme activity. *Cont. Shelf Res.* 28, 2725-2735.

564 Mistic, C., Povero, P., Fabiano, M., 2002. Ectoenzymatic ratios in relation to particulate organic matter
565 distribution (Ross Sea, Antarctica). *Microb. Ecol.* 44, 224–234.

566 Monticelli, L.S., La Ferla, R., Maimone, G., 2003. Dynamics of bacterioplankton activities after a summer
567 phytoplankton bloom period in Terra Nova Bay. *Antarctic Sci.* 15, 85–93.

568 Nelson, D.M., Demaster, D.J., Dunbar, R.B., Smith Jr., W.O., 1996. Cycling of organic carbon and biogenic
569 silica in the Southern Ocean: estimates of water-column and sedimentary fluxes on the Ross Sea
570 continental shelf. *J. Geophys. Res.* 10, 18519–18532.

571 Orsi, A.H., Wiederwohl, C.L., 2009. A recount of Ross Sea waters. *Deep-Sea Res. II* 56, 778-795.
572 doi:10.1016/j.dsr2.2008.10.033

573 Povero, P., Chiantore, M., Mistic, C., Budillon, G., Cattaneo-Vietti, R., 2001. Land forcing controls pelagic-
574 benthic coupling in Adélie Cove (Terra Nova Bay, Ross Sea). *Polar Biol.* 24, 875–882.

575 Povero, P., Mistic, C., Ossola, C., Castellano, M., Fabiano, M., 2003. The trophic role and ecological
576 implications of oval faecal pellets in Terra Nova Bay (Ross Sea). *Polar Biol.* 26, 302–310.

577 Pusceddu, A., Dell’Anno, A., Fabiano, M. 2000. Organic matter composition in coastal sediments at Terra
578 Nova Bay (Ross Sea) during summer 1995. *Polar Biol.* 23:288–293.

579 Rigual-Hernández, A.S., Trull, T.W., Bray, S.G., Closset, I., Armand, L.K., 2015. Seasonal dynamics in diatom
580 and particulate export fluxes to the deep sea in the Australian sector of the southern Antarctic Zone.
581 J. Mar. Syst. 142, 62–74.

582 Rivaro, P., Messa, R., Ianni, C., Magi, E., Budillon, G., 2014. Distribution of total alkalinity and pH in the Ross
583 Sea (Antarctica) waters during austral summer 2008. Polar Res. 33, 20403.
584 <http://dx.doi.org/10.3402/polar.v33.20403>.

585 Rivaro, P., Ianni, C., Langone, L., Ori, C., Aulicino, G., Cotroneo, Y., Saggiomo, M., Mangoni, O., 2015.
586 Physical and biological forcing on the mesoscale variability of the carbonate system in the Ross Sea
587 (Antarctica) during the summer season 2014. J. Mar. Syst., doi: 10.1016/j.jmarsys.2015.11.002.

588 Rossi, S., Isla, E., Martínez-García, A., Moraleda, N., Gili, J.-M., Rosell-Mele, A., Arntz, W.E., Gerdes, D., 2013.
589 Transfer of seston lipids during a flagellate bloom from the surface to the benthic community in the
590 Weddell Sea. Sci. Mar. 77, 397-407. doi: 10.3989/scimar.03835.30A

591 Saggiomo, V., Carrada, G.C., Mangoni, O., Ribera d'Alcalà, M., Russo, A., 1998. Spatial and temporal
592 variability of size-fractionated biomass and primary production in the Ross Sea (Antarctica) during
593 austral spring and summer. J. Mar. Syst. 17, 115–127.

594 Saggiomo, V., Catalano, G., Mangoni, O., Budillon, G., Carrada, G.C., 2002. Primary production processes in
595 ice-free waters of the Ross Sea (Antarctica) during the austral summer 1996. Deep-Sea Res. II 49,
596 1787–1801.

597 Sala, M.M., Arin, L., Balagué, V., Felipe, J., Guadayol, Ò., Vaqué, D., 2005. Functional diversity of
598 bacterioplankton assemblages in western Antarctic seawaters during late spring. Mar. Ecol. Prog. Ser.
599 292, 13–21.

600 Schine, C.M.S., van Dijken, G., Arrigo, K.R., 2016. Spatial analysis of trends in primary production and
601 relationship with large-scale climate variability in the Ross Sea, Antarctica (1997–2013). J. Geophys.
602 Res. Oceans, 121, 368–386, doi:10.1002/2015JC011014.

603 Smith Jr, W.O., Nelson, D.M., Di Tullio, G.R., Leventer, A.R., 1996. Temporal and spatial patterns in the Ross
604 Sea: phytoplankton biomass elemental composition, productivity and growth rates. *J. Geophys. Res.*
605 101, 18455–18466.

606 Smith Jr., W.O., Asper, V.A., 2001. The influence of phytoplankton assemblage composition on
607 biogeochemical characteristic and cycles in the Southern Ross Sea, Antarctica. *Deep-Sea Res. I* 48,
608 137–161.

609 Smith Jr., W.O., Marra, J., Hiscock, M.R., Barber, R.T., 2000. The seasonal cycle of phytoplankton biomass
610 and primary productivity in the Ross Sea, Antarctica. *Deep-Sea Res. II* 47, 3119–3140.

611 Smith Jr., W.O., Dinniman, M.S., Tozzi, S., DiTullio, G.R., Mangoni, O., Modigh, M., Saggiomo, V., 2010.
612 Phytoplankton photosynthetic pigments in the Ross Sea: patterns and relationships among functional
613 groups. *J. Mar. Syst.* 82, 177–185.

614 Soares, M.A., Bhaskar, P.V., Ravidas, R.K., K.Naik, Dessai, D., George, J., Tiwari, M., Anilkumar, N., 2015.
615 Latitudinal $\delta^{13}\text{C}$ and $\delta^{15}\text{N}$ variations in particulate organic matter (POM) in surface waters from the
616 Indian Ocean sector of Southern Ocean and the Tropical Indian Ocean in 2012. *Deep-Sea Res. II* 118,
617 186–196.

618 Spreen, G., Kaleschke, L., Heygster, G., 2008. Sea ice remote sensing using AMSR-E 89 GHz channels. *J.*
619 *Geophys. Res.*, vol. 113, C02S03, doi:10.1029/2005JC003384.

620 Verdugo, P., Alldredge, A.L., Azam, F., Kirchman, D.L., Passow, U., Santschi, P.H., 2004. The oceanic gel
621 phase: a bridge in the DOM–POM continuum. *Mar. Chem.* 92, 67–85.

622 Volkman, J.K., Tanoue, E. 2002. Chemical and biological studies of particulate organic matter in the ocean. *J.*
623 *Oceanogr.* 58, 265–279.

624 Winberg, G.G., 1971. Symbols, units and conversion factors in study of fresh waters productivity. *Int. Biol.*
625 *Programme*, 23.

626 Whitworth T., Orsi, A.H., 2006. Antarctic Bottom Water production and export by tides in the Ross Sea,
627 *Geophys. Res. Lett.* 33, L12609, doi:10.1029/2006GL026357

628 Young, J.N., Goldman, J.A.L., Kranz, S.A., Tortell, P.D., Morel, F.M.M., 2015. Slow carboxylation of Rubisco
629 constrains the rate of carbon fixation during Antarctic phytoplankton blooms. *New Phytol.* 205, 172–
630 181. doi: 10.1111/nph.13021

631 **Captions to figures**

632

633 Fig. 1. A: Map of the stations of the ROME 1 (red dots), ROME 2 (blue dots) and ROME 3 (green dots) areas.
634 Black-circled points indicate the POM sampling stations. B: Θ/S diagram obtained from the entire available
635 dataset indicates the main water masses. Data from the three different areas (ROME 1, ROME 2 and ROME
636 3) are represented with different colours (red, blue and green, respectively).

637

638 Fig. 2. Sea-ice concentration maps of the Ross Sea for 1 December (A), 19 December (B), 7 January (C), 14
639 January (D). Red circles and numbers highlight the position of the ROME 1, ROME 2 and ROME 3 sampling
640 areas.

641

642 Fig. 3. Salinity (left column), temperature (central column) and measured currents (right column) in the
643 upper mixed layer for ROME 1 (A,B,C), ROME 2 (D,E,F) and ROME 3 (G,H,I).

644

645 Fig. 4. Vertical profiles of the variables averaged for each depth at each area (standard deviations are
646 reported). A: particulate organic carbon (POC), B: particulate organic nitrogen (PON), C: particulate organic
647 carbon/particulate organic nitrogen ratio (POC/PON), D: particulate proteins (PRT), E: hydrolysable
648 particulate proteins (h-PRT), F: particulate proteins/carbohydrate ratio (PRT/CHO), G: particulate
649 carbohydrates (CHO), H: hydrolysable particulate carbohydrates (h-CHO), I: particulate lipids (LIP).

650

651 Fig. 5. (A) Contribution of proteins (white), carbohydrates (light grey) and lipids (grey) to POC in the UML
652 (U) and deeper layer (D) for ROME 1, ROME 2 and ROME 3 areas. Black indicates the non-identified fraction
653 of POC, here called "other POC". (B) Average contribution of the hydrolysable fraction of proteins and (C) of
654 the hydrolysable carbohydrates to the POC in the three areas. Standard deviations of POC are reported.
655 Vertical dotted lines: UML, oblique lines: deeper layer.

656

657 Fig. 6. PCA for the entire ROME cruise and the previous studies in the upper mixed layer (UML, coloured
658 markers) and deeper layer (DL, blue markers). Two main groups (A and B) are composed of the sub-groups
659 a1 and a2 (A), b1 and b2 (B). The ellipses are drawn following the results of the cluster analysis on the
660 normalised data (Euclidean distance = 1.8). See text and Table 2 for details. The vectors of the variables are
661 reported on the upper left of the plot.

662

663 Fig. 7. Plot of the POC concentration and caloric value of the POM for the upper mixed layer (A) and the
664 deeper layer (B). Black numbers and markers refer to the previous studies in the Ross Sea and coastal Terra
665 Nova Bay (TNB) (see Table 2 for reference details), red numbers and markers refer to the ROME cruise
666 results. Coloured boxes group the stations that have similar ice-related features (blue: pack-ice coverage,
667 green: marginal ice zone – MIZ, red: polynya) or belong to the coastal sites (violet). See Table 2 for details.

Table(s)

[Click here to download Table\(s\): Misic et al Tables - third revision.docx](#)

668 Table 1. Position of the stations sampled for POM characterisation during the ROME cruise in 2014, depth of the
669 upper mixed layer (UML) and number of sampled depths for each station.

670

	station	date	longitude (°E)	latitude (°S)	UML depth (m)	sampled depths
ROME 1	9	16 Jan	173.87	75.00	38	5
	11	16 Jan	172.03	75.00	29	5
	13	16 Jan	170.76	75.00	32	5
	16	17 Jan	169.50	74.83	15	5
	18	17 Jan	169.51	74.51	17	5
	20	17 Jan	169.88	73.99	14	5
ROME 2	33	26 Jan	166.06	74.70	18	4
	34	26 Jan	165.75	74.76	13	5
	36	27 Jan	165.18	74.88	12	5
	39	27 Jan	166.06	74.86	24	4
	43	27 Jan	164.98	74.79	14	4
	45	28 Jan	165.49	74.82	15	5
ROME 3	48	31 Jan	167.83	76.40	33	5
	50	31 Jan	168.65	76.40	36	5
	52	1 Feb	169.53	76.42	75	4
	55	1 Feb	168.40	76.43	44	5
	56	1 Feb	168.16	76.54	12	5
	65	2 Feb	169.58	76.50	115	4
	67	2 Feb	168.72	76.50	51	5
	69	2 Feb	168.01	76.50	14	4
75	3 Feb	168.80	76.38	42	5	

671

672 Table 2. Features of the stations sampled during previous researches, here used as a comparison for the ROME
 673 cruise observations.

674

area	season	environmental features	station	lat °S	long °E	reference
Ross Sea	spring	polynya	MP	76.50	175.00	Fabiano et al. (2000)
		MIZ	8	75.16	175.18	
		MIZ	10	74.84	174.88	
		MIZ	28	74.70	172.01	
		MIZ	30	74.69	164.18	
		pack	27	71.94	174.98	
	pack	29	74.98	167.99		
	early summer	polynya	15	72.35	179.78	Fabiano et al. (1993); Catalano et al. (1997)
		polynya	17	73.23	179.84	
		polynya	19	74.95	179.82	
		polynya	21	74.98	174.87	
		MIZ	23	74.99	170.00	
MIZ		25	74.95	165.25		
Terra Nova Bay	summer	coastal-open waters	TNB	74.78	164.17	Povero et al. (2001)
			TNBa	74.75	164.17	Fabiano et al. (1995)
			TNBb	74.70	164.13	Fabiano et al. (1997)

675

Table 3. Significant correlations between the different variables for each area investigated during the ROME cruise. Underlined numbers: $p < 0.05$, normal numbers: $p < 0.01$, bold numbers: $p < 0.001$. The number of observation varied in the three Legs: in ROME 1 chlorophyll-a showed 13 observations, hydrolysable carbohydrate and lipid 18, the other variables 28. In ROME 2 they were: 19, 12 and 25, respectively. In ROME 3: 25, 13 and 40, respectively.

		Chl-a	PON	POC	PRT	h-PRT	CHO	h-CHO
ROME 1	PON	0.68						
	POC	0.72	1.00					
	prt	0.73	0.99	1.00				
	h-PRT	0.76	0.94	0.95	0.97			
	CHO	0.71	0.97	0.98	0.98	0.94		
	h-CHO	-	0.76	0.75	0.77	0.83	0.82	
	LIP	<u>0.63</u>	0.89	0.92	0.91	0.90	0.88	0.65
ROME 2	PON	-						
	POC	-	0.96					
	prt	-	0.97	0.95				
	h-PRT	-	0.89	0.90	0.94			
	CHO	0.65	0.68	0.81	0.77	0.79		
	h-CHO	-	-	-	-	-	0.72	
	LIP	-	-	-	-	-	<u>0.53</u>	<u>0.63</u>
ROME 3	PON	0.95						
	POC	0.95	0.99					
	prt	0.95	0.99	0.99				
	h-PRT	0.86	0.93	0.94	0.94			
	CHO	0.90	0.93	0.95	0.94	0.91		
	h-CHO	<u>0.64</u>	0.74	0.74	0.74	0.72	0.80	
	LIP	0.68	0.91	0.91	0.90	0.90	0.89	0.68

Chl-a: chlorophyll-a, PON: particulate organic nitrogen, POC: particulate organic carbon, PRT: proteins, h-PRT: hydrolysable proteins, CHO: carbohydrates, h-CHO: hydrolysable carbohydrates, LIP: lipids.

Table 4. Multivariate statistical analysis (ANOSIM and SIMPER) for the two main groups A and B of the PCA (Fig. 6) and the sub-groups a1-a2 and b1-b2. Mean values \pm standard deviation for each group and sub-group are reported (Particulate Organic Carbon (POC), proteins (PRT) and carbohydrates (CHO): $\mu\text{g l}^{-1}$; protein/carbohydrate ratio (PRT/CHO): $\mu\text{g } \mu\text{g}^{-1}$).

groups	ANOSIM		SIMPER			
	R statistic	significance	variable	%	average \pm sd	average \pm sd
A vs B	0.847	0.1 %	PRT	32	A: 281.4 \pm 62.9	B: 58.8 \pm 47.5
			PRT/CHO	25	3.6 \pm 1.0	2.1 \pm 0.9
			CHO	24	90.0 \pm 32.9	32.7 \pm 30.0
			POC	19	242.8 \pm 55.0	72.4 \pm 53.9
a1 vs a2	0.656	0.1 %	PRT/CHO	41	a1: 4.3 \pm 0.7	a2: 2.9 \pm 0.4
			CHO	36	63.1 \pm 15.7	115.1 \pm 23.0
			PRT	14	243.8 \pm 60.1	316.4 \pm 43.0
b1 vs b2	0.903	0.1 %	CHO	47	b1: 15.9 \pm 5.5	b2: 71.5 \pm 27.1
			PRT/CHO	22	2.2 \pm 1.0	1.7 \pm 0.4
			POC	17	40.7 \pm 14.4	145.7 \pm 36.6
			PRT	14	33.2 \pm 17.1	118.0 \pm 41.8

Figure 1
[Click here to download high resolution image](#)

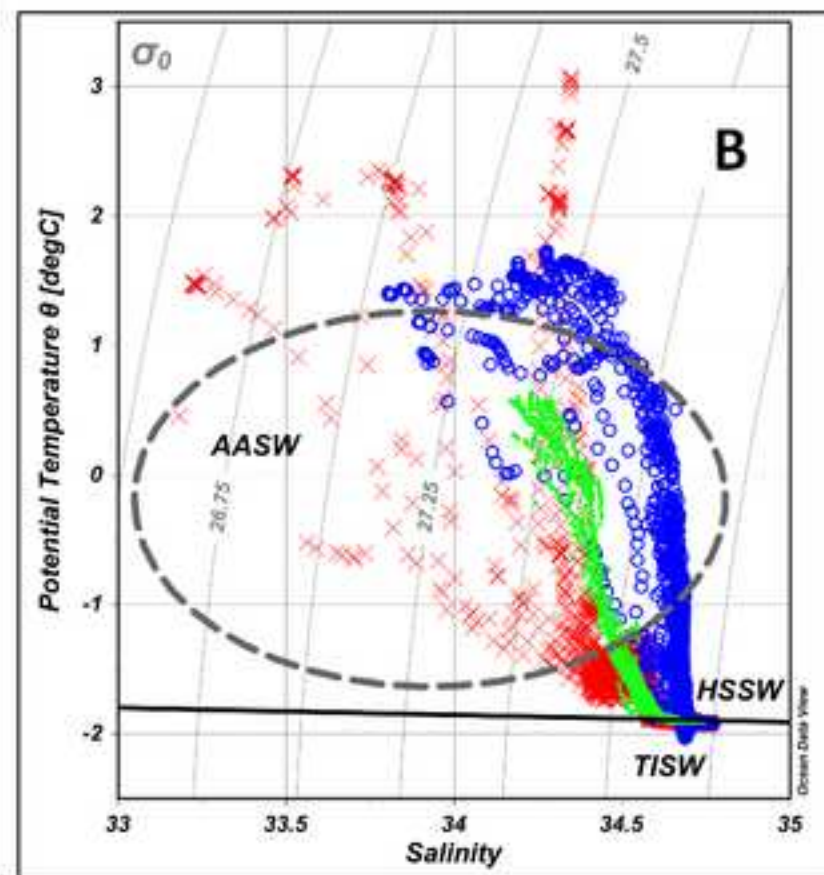
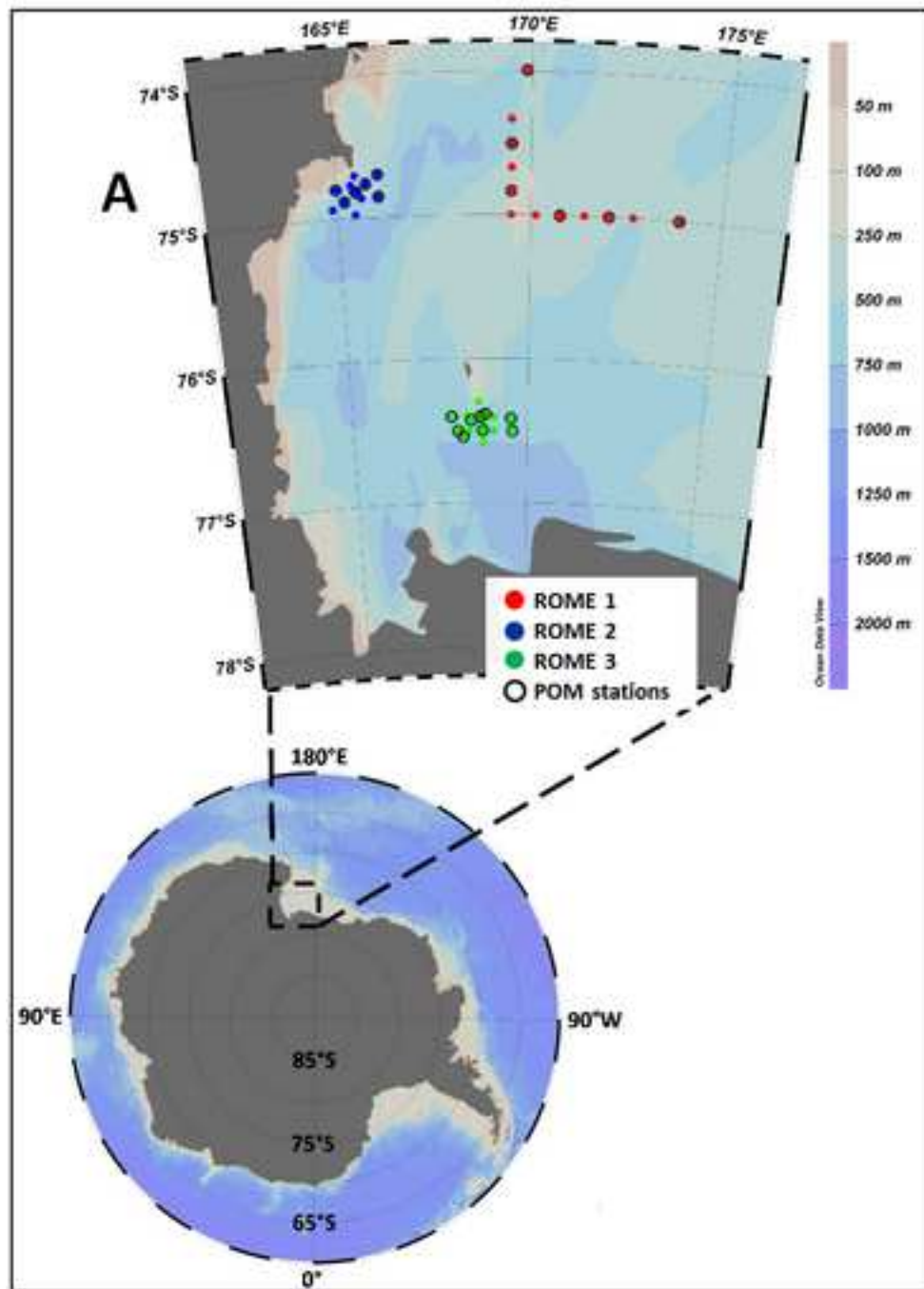


Figure 2

[Click here to download high resolution image](#)

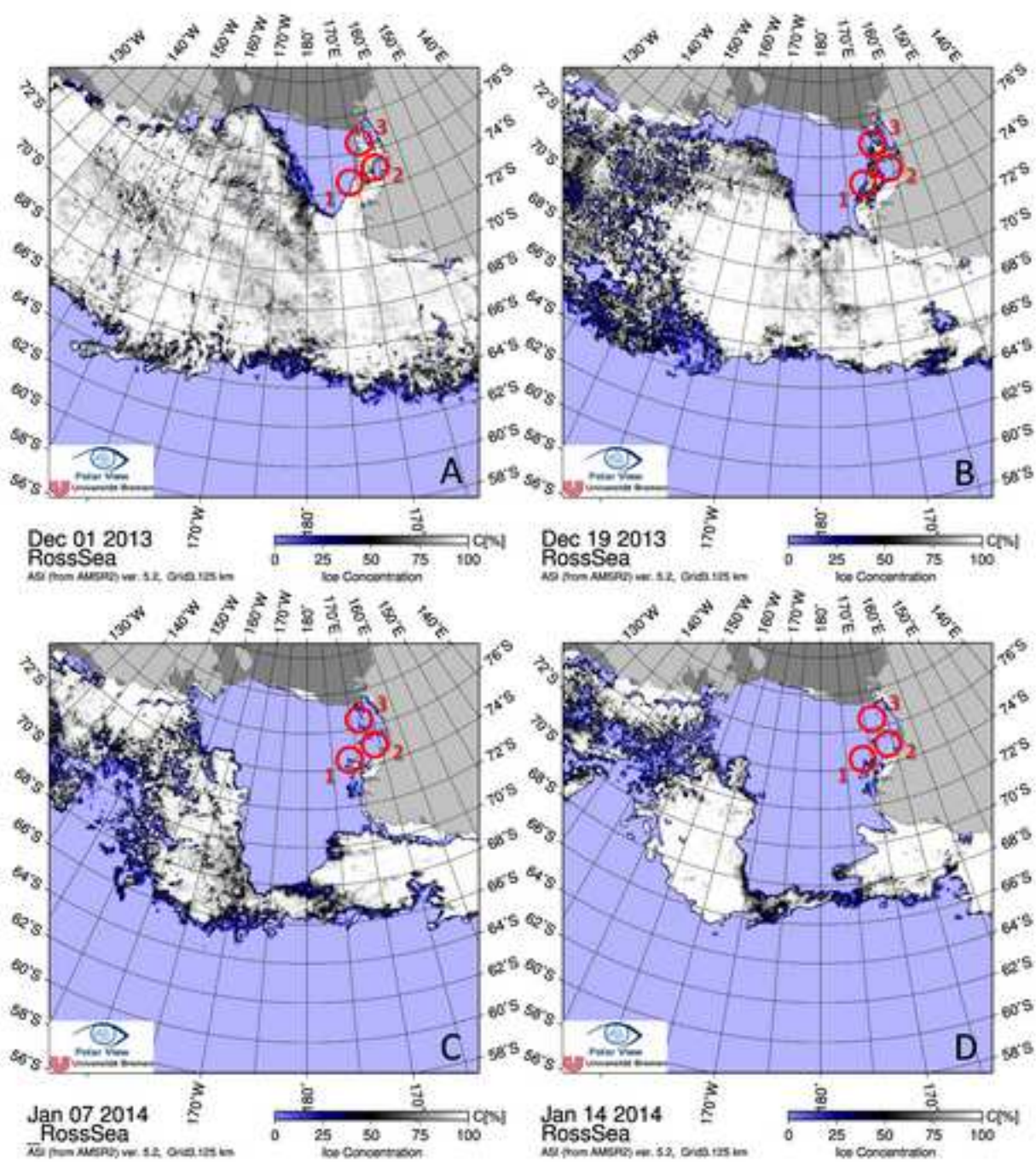


Figure 3
[Click here to download high resolution image](#)

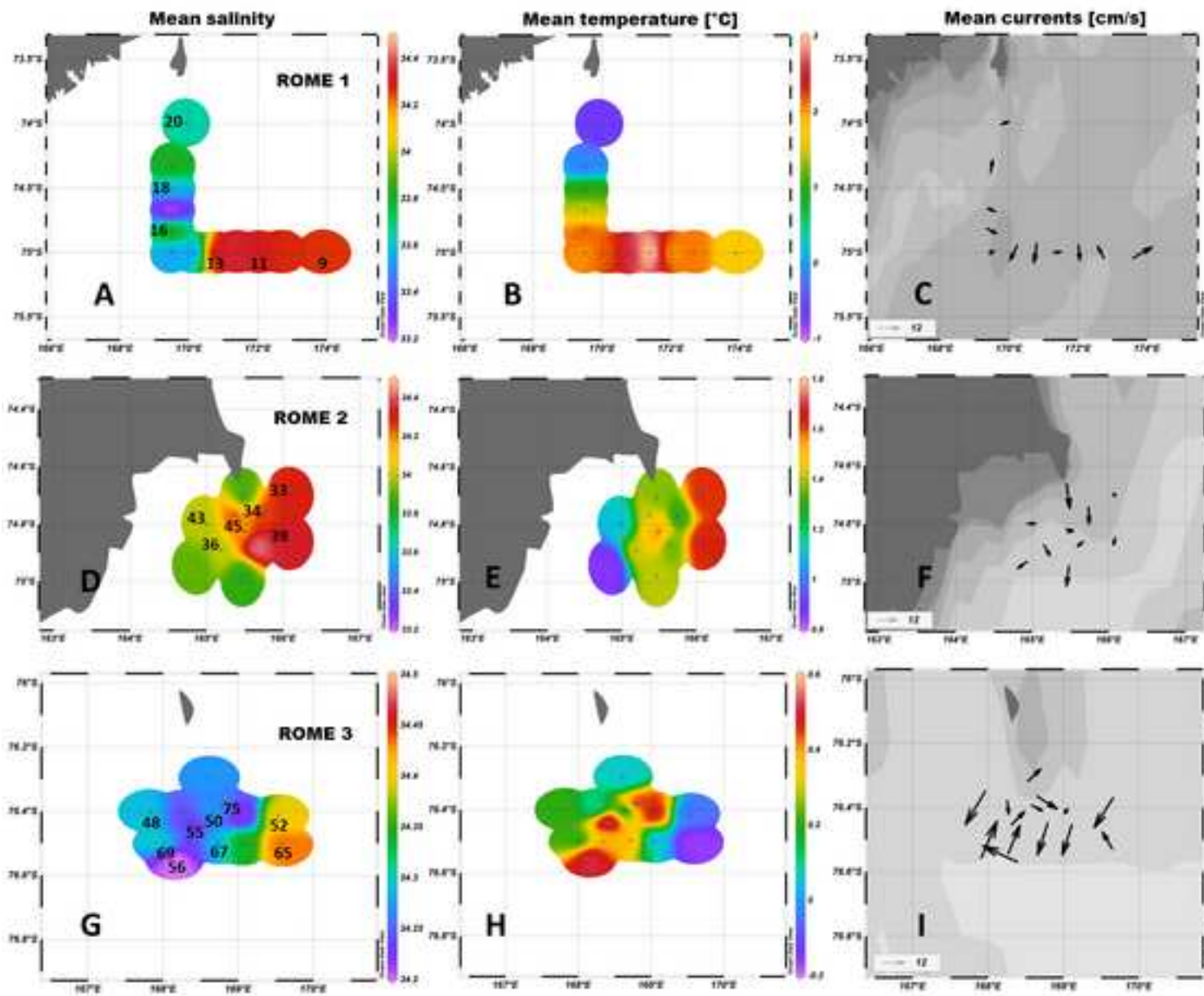


Figure 4
[Click here to download high resolution image](#)

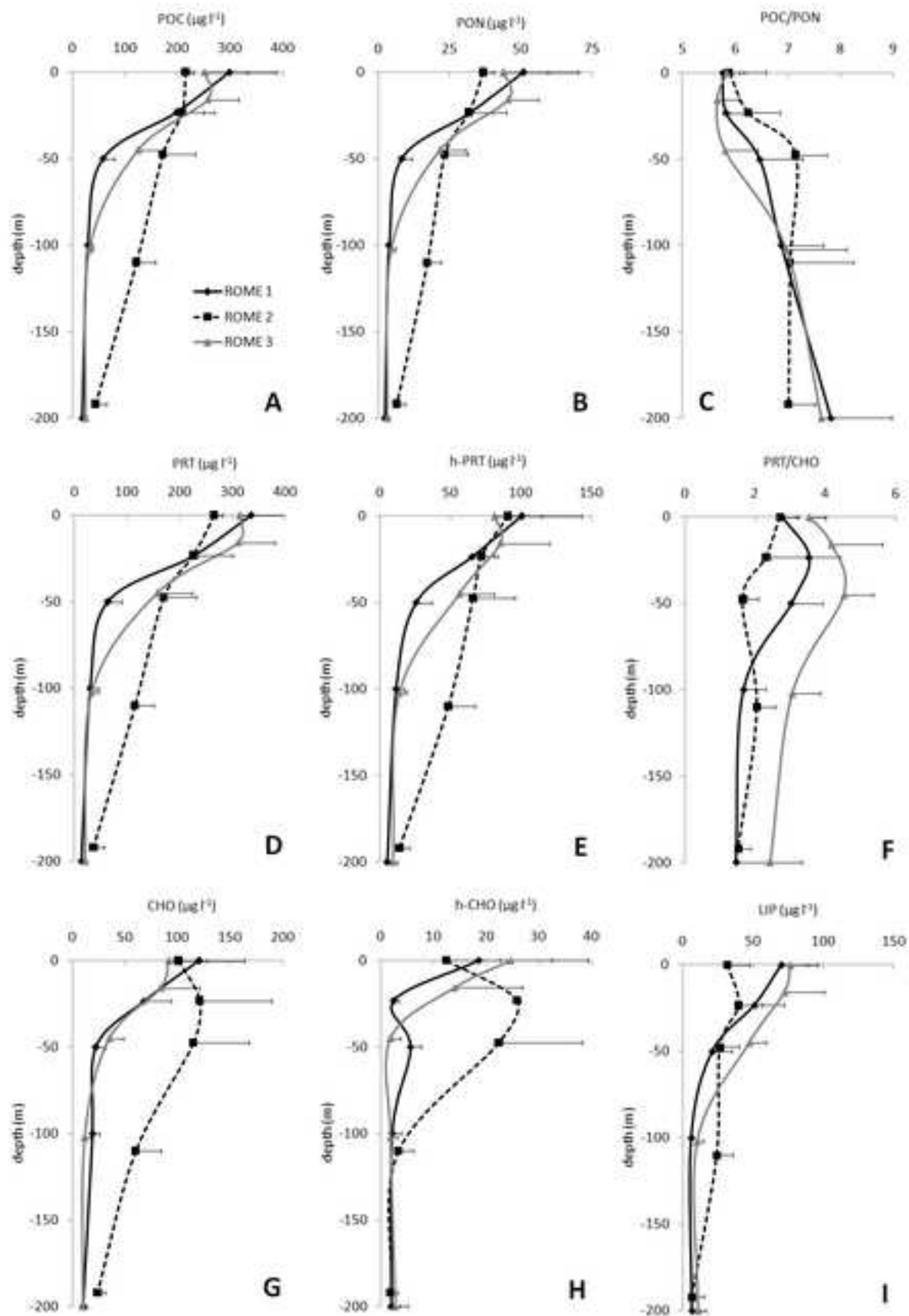


Figure 5
[Click here to download high resolution image](#)

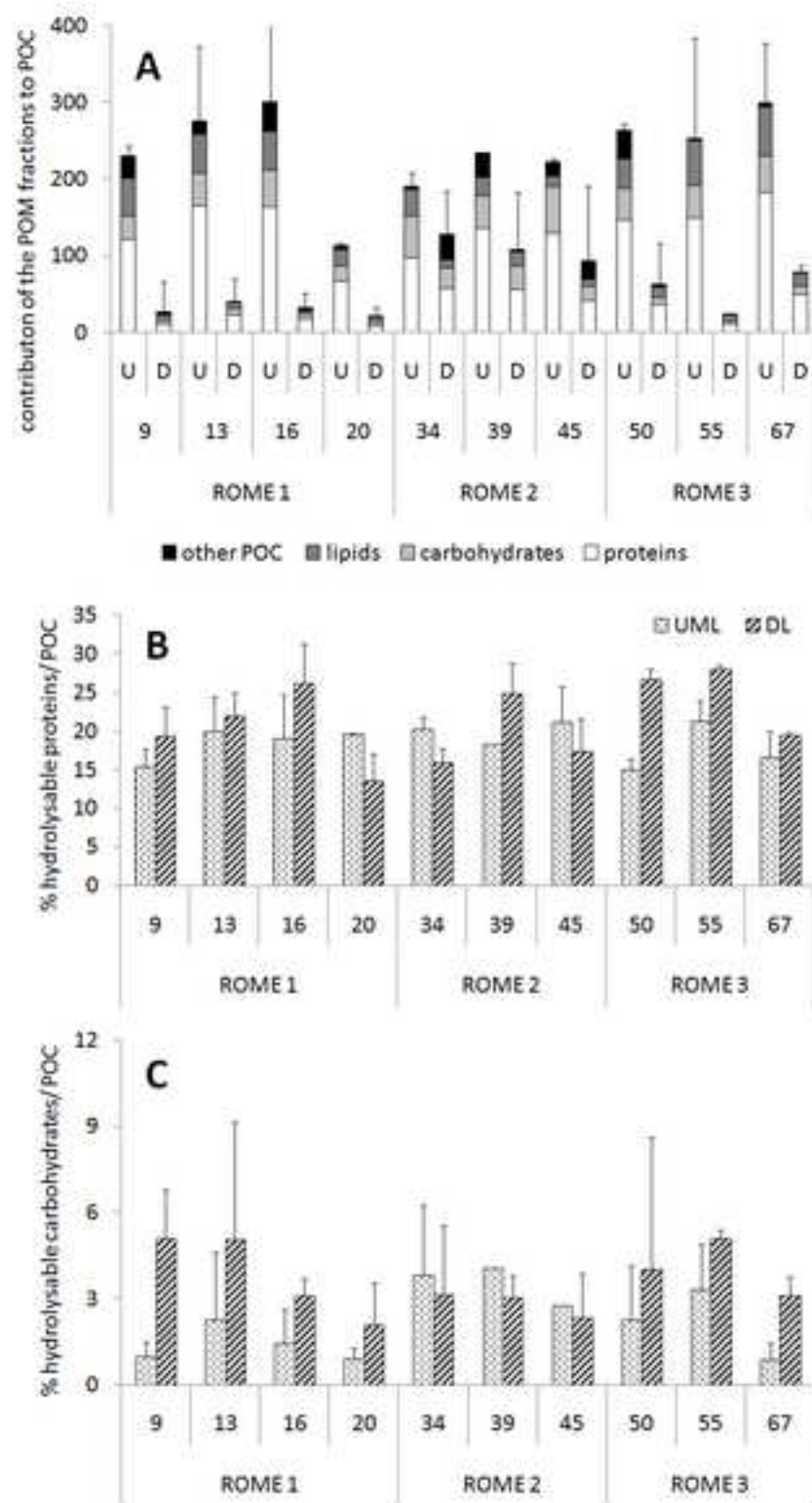
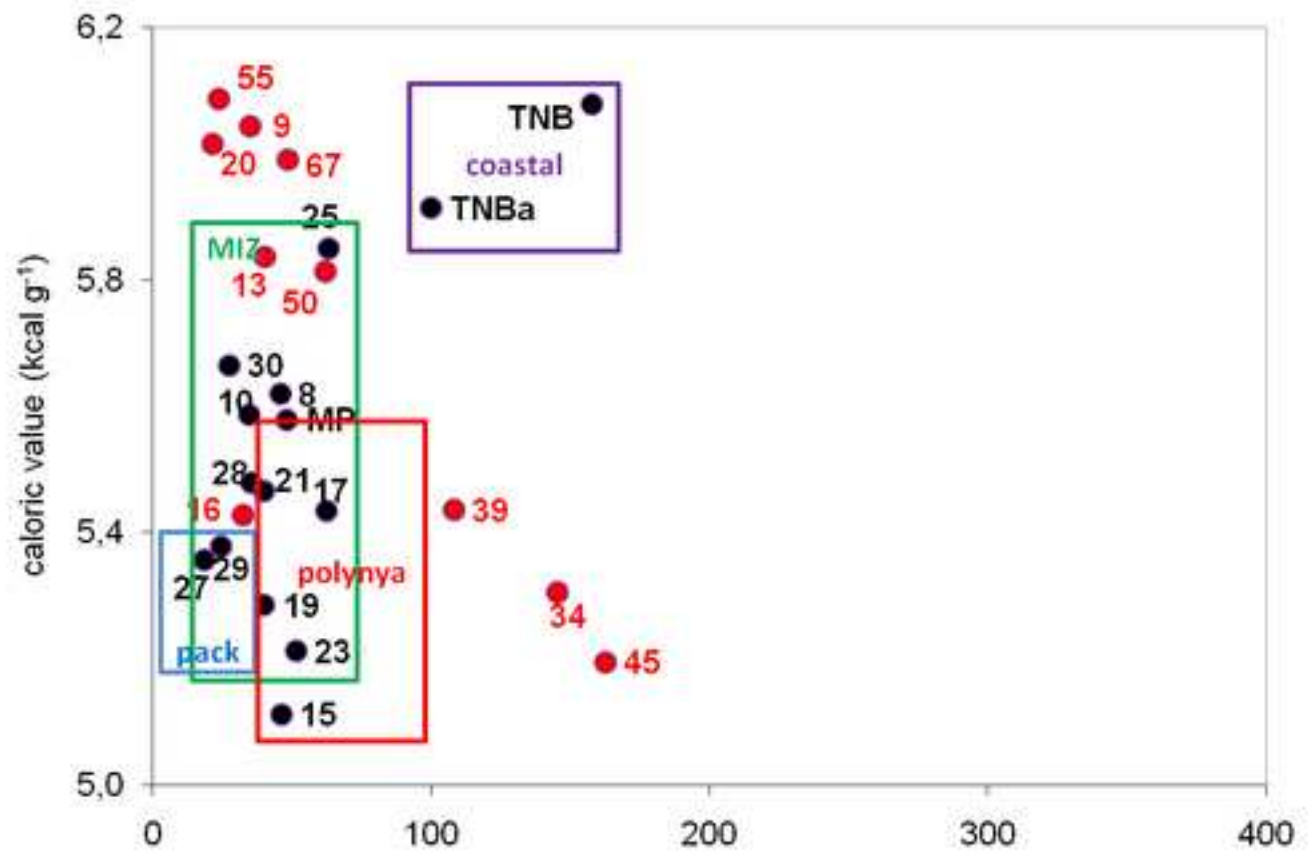
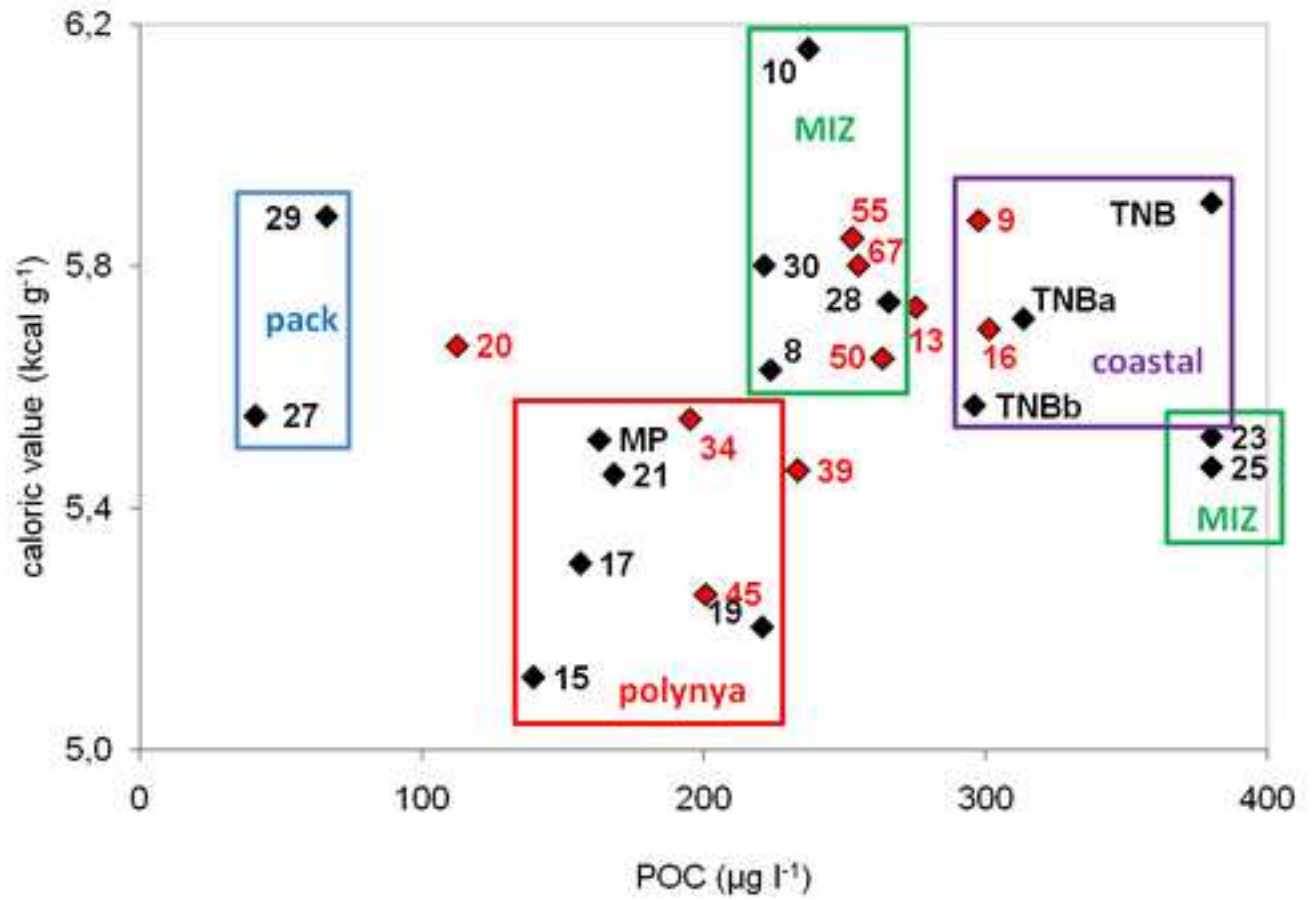


Figure 7
[Click here to download high resolution image](#)



Supplementary material for online publication only

[Click here to download Supplementary material for online publication only: Table Appendix.docx](#)